Biofabrication

International Society for Biofabrication

PAPER • OPEN ACCESS

Three-dimensional cartilage tissue regeneration system harnessing goblet-shaped microwells containing biocompatible hydrogel

To cite this article: Nopphadol Udomluck *et al* 2020 *Biofabrication* **12** 015019

Biofabrication

OPEN ACCESS

RECEIVED
29 July 2019

REVISED
25 October 2019

ACCEPTED FOR PUBLICATION
29 November 2019

PUBLISHED
23 December 2019

PAPER

Three-dimensional cartilage tissue regeneration system harnessing goblet-shaped microwells containing biocompatible hydrogel

Nopphadol Udomluck[1,3], **Sung-Hwan Kim**[2,3], **Hyunjoo Cho**[1], **Joong Yull Park**[2,4] and **Hansoo Park**[1,4]

[1] School of Integrative Engineering, College of Engineering, Chung-Ang University, Seoul 06974, Republic of Korea
[2] School of Mechanical Engineering, College of Engineering, Chung-Ang University, Seoul 06974, Republic of Korea
[3] These authors contributed equally to the work.
[4] Authors to whom any correspondence should be addressed.

E-mail: jrpark@cau.ac.kr and heyshoo@cau.ac.kr

Keywords: spheroid culture, osteochondral tissue, chondrogenic, goblet-shaped microwell

Supplementary material for this article is available online

Abstract

Differentiation of stem cells into chondrocytes has been studied for the engineering of cartilage tissue. However, stem cells cultured two-dimensionally have limited ability to differentiate into chondrocytes, which led to the development of three-dimensional culture systems. A recently developed microtechnological method uses microwells as a tool to form uniformly sized spheroids. In this study, we fabricated an array (10 × 10) of goblet-shaped microwells based on polydimethylsiloxane for spheroid culture. A central processing unit (CPU) was used to form holes, and metallic beads were used to form hemispherical microwell geometry. The holes were filled with Pluronic F-127 to prevent cells from sinking through the holes and allowing the cells to form spheroids. Viability and chondrogenic differentiation of human adipose-derived stem cells were assessed. The fabrication method using a micro-pin mold and metallic beads is easy and cost-effective. Our three-dimensional spheroid culture system optimizes the efficient differentiation of cells and has various applications, such as drug delivery, cell therapy, and tissue engineering.

1. Introduction

Osteochondral tissue is a complex tissue that includes both chondrogenic and osteogenic cells. Defective osteochondral tissue causes osteoarthritis, affecting millions of people worldwide [1]. Osteochondral defects refer to degeneration of both the articular cartilage and a piece of underlying subchondral bone [2]. To repair the defect, the complexity of the bone and cartilage must be considered, as the development of osteochondral regeneration has been slowed by technical obstacles related to its complex and hierarchical architecture [3]. In osteochondral tissue, the bone and cartilage exist in different matrices and biophysical environments, which are associated with the transport of molecules. Moreover, the three-dimensional (3D) arrangement of chondrogenic cells in the native osteochondral tissue is challenging to imitate *in vitro* [4]. To achieve this, scaffolds should mimic the 3D *in vivo* condition of osteochondral tissue [5–7]. The 3D environment can induce the chondrogenic phenotype by promoting cell-matrix interactions with the collagen fiber network and the rest of the intercellular protein matrix [5]. As osteochondral tissue is composed of a 3D structure of collagen matrix and proteoglycans, various 3D culture methods have been applied to the regeneration of osteochondral tissue [8–11].

Spheroid culture is one of the most specialized methods for the 3D cultivation of cells. It has been explored for various applications in tissue engineering [6, 12–14]. Spheroids are spherical cell aggregates that can self-organize through interaction with surrounding cells or extracellular matrix. Spheroid technology has been explored with adipose stem cells or human mesenchymal stem cells (hMSCs) to test chondrogenic differentiation and tissue function, and to reveal cellular functions [15–18]. In addition, spheroid preparation methods, such as the use of microwells or micropatterns, have been introduced [6, 16, 19]. These

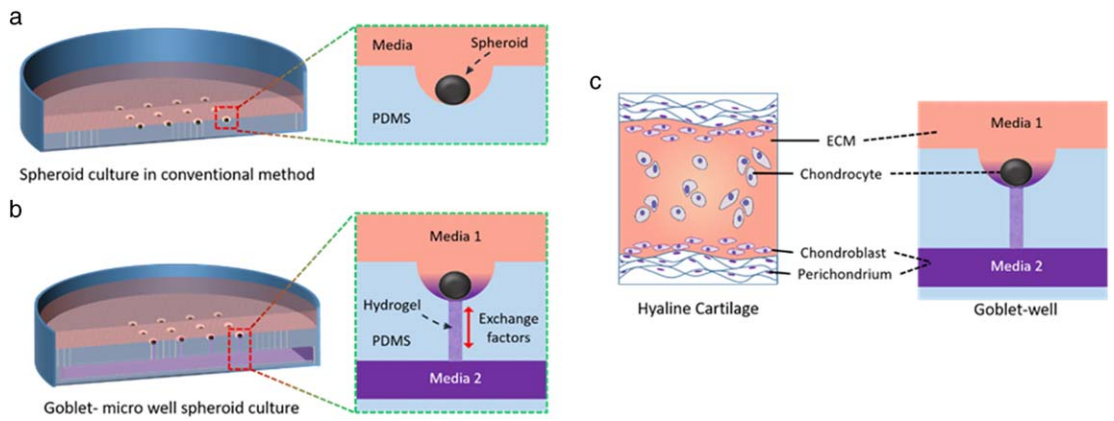

Figure 1. Concept of the goblet-well. (a) In conventional microwells, it is difficult to dynamically supply biochemical molecules to spheroids using various media. (b) The goblet-well can be exposed to two different media by adding a hole filled with hydrogel to the existing microwell. (c) The goblet-well compared with chondrogenic cells in hyaline cartilage illustration [24]. Abbreviations are: PDMS: polydimethylsiloxane, and ECM: extracellular matrix.

studies have shown that cells cultured in a micro-sized system form dense spheroids that remain relatively constant in size.

Although microwell arrays allow the spontaneous formation of spheroids (figure 1(a)), additional elements are required to mimic specific organisms and tissues. In particular, the supply of various cytokines and nutrients and interaction with other cell types that determine cell differentiation can be provided on advanced platforms [20]. The microfluidic system allows selective cell seeding in microwells so that different cells can be seeded into the desired array in the microwells [21], which enables spheroid co-culture by connecting a microwell to another cell culture chamber [22]. With this system, hepatocyte and hepatic stellate cells were cultured to mimic the environment of liver tissue. However, these microfluidic systems require sophisticated cell seeding controls and additional experiments to fabricate microchannels. Studies have mimicked various biological environments through co-culture in microwells without using microfluidic systems. Hair follicle stem cells, fibroblasts, and keratinocytes were co-cultured to mimic the hair follicle environment and thus produce new hair in microwells [23]. However, spheroids in the microwell arrays introduced in the earlier studies were not exposed to multiple cytokines. Considering that the exposure of cells to various biochemical components in the 3D microenvironment is a biological norm, it is important to develop systems capable of mimicking this exposure.

Here, we have developed a novel goblet-shaped microwell (goblet-well) system that can expose spheroids to two different types of biochemical stimuli/nutrients (figure 1(b)) mimicking the physiological environment of osteochondral tissue. The system permits the easy replacement of the two different media at the desired time. Furthermore, the diffusion time can be controlled according to the type of hydrogel. The biomimetic benefits of this system include 3D cell culture (spheroid), multi-stimuli capability, and the ability to expand to accommodate co-culture systems. The goblet-well consists of a microscale hemispherical well in which a spheroid is cultured. A through-hole filled with hydrogel (Pluronic F-127) helps diffusive exchange of the biochemical molecules of the medium in the bottom layer, and supports spheroid formation by reducing cell adhesion to the surface and preventing the cells sinking through the hole [25–27]. As a demonstration, we cultured human adipose-derived stem cells (hASCs) for 14 d in this goblet-well array and observed the differentiation of the hASCs into chondrocytes.

Goblet-wells filled with hydrogel are relevant for drug research because they provide an *in vivo*-like chondrogenic tissue model (figure 1(c)) that features the intercellular interaction and the transfer of multiple cytokines, such as interleukins, fibroblast growth factor, and bone morphogenic proteins [28]. This system can provide a higher-level simulation of *in vivo* -like conditions, and thus can be useful for drug screening, stem cell differentiation research, and other fundamental physiology related studies.

2. Methods

2.1. Fabrication of polydimethylsiloxane (PDMS) goblet-wells

The goblet-well substrate was made of PDMS (Dow Corning Inc., USA). Each well has a hemispherical microstructure with a diameter of 600 μm that is connected to the bottom through a 300 μm diameter hole (figure 2). To fabricate the 3D goblet-shaped microstructure, the micro-pin array and conventional central processing units (CPUs) with a pin diameter of 0.3 mm and height of 1.8 mm obtained from a CPU processor (AMD Athlon, USA) were used as a micro-pillar array mold. The CPU pin array was placed in a

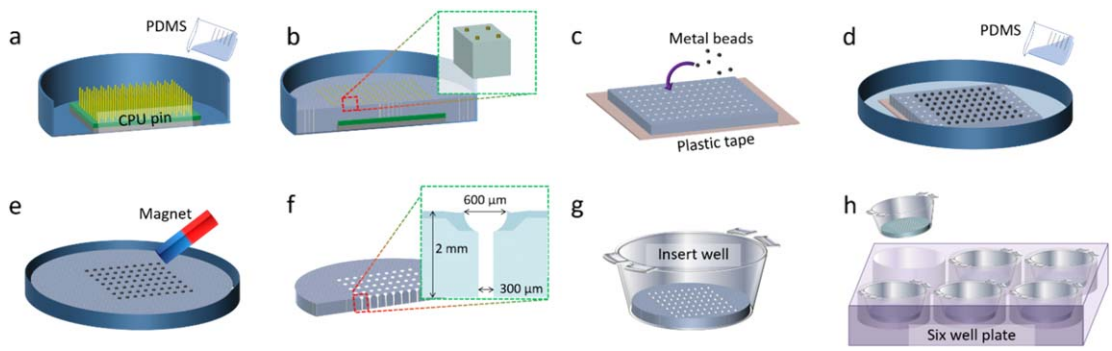

Figure 2. Goblet-well fabrication process. (a) CPU pins are placed in a petri dish and the PDMS solution is poured over the array. (b) The volume of PDMS is adjusted at the top-end of each CPU pin and then solidifies to form the PDMS mold. (c) The solidified PDMS is separated from the CPU pins, and attached to a piece of plastic tape to cover the bottom of the hole. The 600 μm metal beads are placed on the tape. (d) After heating the PDMS with the metal beads at 100 °C for 10 min and bringing it to room temperature, the PDMS solution is poured to fill the middle part of the bead and is solidified at room temperature for one day. (e) The metal beads are removed from the solidified PDMS using a magnet. (f) The completed goblet-well array. The size of the hemispherical well is determined by the bead size; the diameter of the hole is 300 μm and the total height is 2 mm. (g) The goblet-well array is adhered to the insert well using PDMS glue (PDMS solution). (h) Using the prepared insert wells and six-well plates, spheroid cells are cultured using two different culture media.

10 mm diameter petri dish (figure 2(a)). PDMS solution mixed with base and curing agent (SYLGARD 184; Dow Corning) in a ratio of 10:1 was added. The volume of liquid PDMS added was adjusted so the level of the solution came to the top-end of the CPU pins without immersing them (figure 2(b)). After curing in an oven at 80 °C for 2 h, the PDMS substrate was removed from the CPU pins to produce a flat rectangular PDMS substrate with an array of micro-holes. The bottom of the obtained substrate was sealed with plastic tape, and 600 μm diameter metal beads were aligned on the upper surface of each hole to prepare the goblet shape of the well (figure 2(c)). To immobilize the bead on the top of a hole, thermal expansion/contraction was used as follows. When the system was heated at a high temperature (approximately 100 °C), the air in the holes expanded. After 10 min, the temperature was allowed to decrease to room temperature. The air inside each hole contracted, which secured the beads in place by the negative pressure created in the hole. This thermal expansion/contraction of trapped air in the hole follows Charles's law ($V_T = V_0(1 + T/273)$), where V_T is the volume of gas at temperature T and V_0 is the volume at 0 °C. After that, additional PDMS solution was poured to half the height of the beads and cured at room temperature for one day (figure 2(d)). The PDMS thickness has been controlled in other studies using spin-coating [29, 30]. However, this method cannot be applied in this system since the beads are fixed in place. Instead, we controlled the thickness of the poured PDMS by tilting the substrate and allowing excess PDMS to flow off. The beads were then removed and collected using a neodymium magnet (figure 2(e)) to generate the goblet-wells (figure 2(f)). By removing the plastic tape, a goblet-shaped microwell array was obtained. The uniform goblet-wells were characterized using SEM (S3400N, Hitachi, Japan). For cell culture, 10 × 10 goblet-well arrays were cut and attached to the insert well (figure 2(g)). A six-well plate was typically used for co-culture (figure 2(h)).

2.2. Filling goblet-well holes with Pluronic F-127

To ensure stable formation of the spheroids, the holes connected to the goblet-wells were filled with a solution of Pluronic F-127 (P2443; Sigma-Aldrich, USA). To prepare the solution, Pluronic F-127 powder was added slowly to cold Dulbecco's phosphatebuffered saline (DPBS) at 4 °C (using an ice bath) and stirred at 900 rpm for 1 d. The Pluronic gel F-127 concentration of 30% w/v was poured into the 10 × 10 goblet-wells and allowed to drain through the hole, still at 4 °C. When the Pluronic F-127 solution had completely drained, it was dried in a dry oven at 40 °C for 1 d. Wells were confirmed to be filled with gel by optical microscopy using an ECLIPSE TS100 microscope (Nikon, Japan) at ×4 and ×10 magnification. Moreover, the presence of gel was validated by safranin-O dye. Briefly, safranin-O solution, 1%w/v was added to the goblet-wells. After drying the gel, both side of the hole was exposed with DPBS. Then images were captured using a microscope (Olympus 110AL2X-2, Japan) mounted with a DSLR camera (Canon EOS 600D, Japan). For better visualization, the goblet-well was observed in a vertically cut cross-section view.

2.3. Diffusion through the holes

The spheroids cultured in the goblet-wells are exposed to two different media supplied from the top and bottom layers. The bottom layer medium is transported by diffusion through the Pluronic gel that fills the hole (figure 4). It was necessary to quantitatively confirm the diffusion rate of the bottom layer medium

(biochemical) to the spheroids. To visualize the diffusion inside the hole, Trypan blue was used to fill the bottom layer as a dye reagent. The movement of the dye in the hole was observed in real-time and photographed with a microscope. The goblet-well was cut vertically from top to bottom, and the diffusion that had occurred on the central axis of the hole was observed. Experiments were carried out in the presence of 30% Pluronic F-127 in the hole.

2.4. Diffusion simulation model

Computational geometry of a goblet-well was constructed and a 3D diffusion simulation was performed. The dimensions used in the analysis were the same as in the fabricated goblet-wells. The microwell and hole diameter were 600 μm and 300 μm, respectively, and the distance from the bottom to the goblet-well was 2 mm. A 100% mass fraction of the bottom medium was set as the source term for the bottom surface of the hole. A 1 mm square columnar domain above the microwell was set to serve as the culture medium for which the diffusion of cytokines from the bottom of the hole to the outside was calculated. The software used in this simulation was ANSYS Fluent 15 (Ansys Inc., USA). The goblet-well was assumed to be filled with water (a homogeneous, incompressible Newtonian fluid) at 36 °C and the bottom of the hole was fixed with another water medium. Two different types of water media mixed through diffusion, where the diffusion coefficient (1×10^{-10} $m^2 s^{-1}$) [31] of a cytokine was applied. There were 300 000 grids, and the time step size was 1 s.

2.5. hASC spheroid culture

The hASCs were isolated from adipose tissue obtained during surgeries conducted at the Korea Cancer Center Hospital. The hASCs were expanded up to passage 5 using low-glucose Dulbecco's modified Eagle's medium (DMEM-LG; HyClone, USA) containing 1% antibiotic/antimycotic solution (HyClone) and 10% fetal bovine serum (FBS; HyClone). The medium was replenished every 2 d. The cultured cells were harvested using 0.25% trypsin (1×) solution (HyClone). The harvested cells were seeded at a concentration of 0.5×10^6 cells ml^{-1} on the PDMS substrate (5000 cells in each goblet-well). Cells that did not enter the goblet-wells were removed by carefully aspirating the medium. Then the substrate was refilled with the fresh medium. The hASCs from passage 5 were incubated in a humidified incubator at 37 °C and 5% CO_2. The formation of spheroids was confirmed by optical microscopy using the aforementioned ECLIPSE TS100 microscope. The diameters of the spheroids in the micrographs were measured using the ImageJ software (v. 1.48, National Institutes of Health, USA).

2.6. Cell viability analysis

The viability of hASC spheroids cultured in goblet-wells was analyzed using the LIVE/DEAD Viability/Cytotoxicity kit for mammalian cells (Molecular Probes, USA) at days 1, 3, 7, and 14. Spheroids were rinsed using DPBS for 20 min to remove the medium and the kit solution (4 mM calcein AM and 2 mM ethidium homodimer in DPBS) was added to each goblet-well and incubated at 37 °C and 5% CO_2 for 30 min. The stained cells were observed by fluorescence microscopy using a model OX.2053-PLPH microscope (Euromax, Netherlands). Moreover, anoikis propelled cell death was confirmed by anoikis assay detection kit (Abcam, UK) following fluorometric detection method in kit manual. Briefly, 1 μl of ethidium homodimer (500×) was added to 96-well plate having 4 d cultured spheroid samples. The plate was then incubate at 37 °C for 30 min and the signals were measured using microplate reader (Biotek Instruments, USA) at 525 nm excitation wavelength and 590 nm emission wavelength.

2.7. Cell spheroid proliferation tests

The proliferation of hASC spheroids cultured in the goblet-wells was measured using the CCK-8 assay (Dojindo Molecular Technologies, USA) compared to conventional microwells, after culture for 1, 3, and 7 d. CCK-8 solution was added to the medium and adjusted to 10% of the total medium volume in each goblet-well. After incubation for 3 h, 100 μl of the medium was collected from each well to check the absorbance at 450 nm using a Synergy H1 multi-mode microplate reader (Biotek Instruments, USA). The obtained absorbances were used to calculate cell quantity by comparison with the standard curve. The quantities obtained with time allowed determination of cell proliferation.

2.8. Chondrogenic differentiation and gene expression analysis

The hASCs were cultured in the goblet-well array with general medium (GM) including DMEM-LG containing 1% antibiotic/antimycotic solution (HyClone) and 10% FBS for 3 d to allow spheroid formation. Then, spheroids were supplied with chondrogenic differentiation medium (CDM) that contained 50 $\mu g\ ml^{-1}$ ascorbic acid (Sigma-Aldrich), 10 mM Insulin-Transferrin-Selenium-A (100×; Gibco, USA), 0.01 μM dexamethasone (Sigma-Aldrich), and 10 $\mu g\ ml^{-1}$ transforming growth factor-beta 1 (TGF-β1; ProSpec, Israel). The hASCs were cultured for up to 14 d. After 7 and 14 d, the chondrogenic differentiation of cells was measured using gene expression analysis with real-time quantitative PCR (RT-qPCR). To compare with the conventional culture method, the goblet-well array spheroid culture was compared with a conventional microwell culture (3D cell culture kit organoid-well, Cellsmith Inc., Republic of Korea). To investigate the efficiency of diffusion of the

Table 1. RT-qPCR primer sequences for analysis of chondrogenic differentiation. Abbreviations are: F, forward primer; R, reverse primer; GAPDH, glyceraldehyde-3-phosphate dehydrogenase; AGG, Aggrecan; COL2, collagen type II; and SOX9, transcription factor SOX-9.

Gene	Sequence
GAPDH	F 5′ ACA TCG CTC AGA CAC CAT G 3′
	R 5′ TGT AGT TGA GGT CAA TGA AGG G 3′
AGG	F 5′ GCC TGC GCT CCA ATG ACT 3′
	R 5′ ATG GAA CAC GAT GCC TTT CAC 3′
COL2	F 5′ CAC GTA CAC TGC CCT GAA GGA 3′
	R 5′ CGA TAA CAG TCT TGC CCC ACT T 3′
SOX9	F 5′ CCC CAA CAG ATC GCC TAC AG 3′
	R 5′ GAG TTC TGG TCG GTG TAG TC 3′

goblet-well array, four different sample conditions related to the location of the medium were tested. The first condition (GM/GM) involved GM in the upper and lower parts of the goblet-well substrate. The second condition (GM/CDM) and third condition (CDM/GM) involved CDM (double concentration of normal concentration) in the lower and upper parts of the substrate, respectively. The fourth condition (CDM/CDM) involved CDM (X1 concentration) in the upper and lower parts of the substrate.

For gene expression analysis, hASC spheroids in each goblet cell were rinsed using DPBS and the total mRNA was isolated using Trizol reagent (Thermo Fisher Scientific, USA). The isolated total mRNA concentration was quantified using a microplate reader by determining the ratio of the absorbances at 260 nm and 280 nm. An equal amount of cDNA was synthesized in 10 μl of RT-PCR mixture containing RNA template, random hexamer, 5× PrimeScript™ Buffer, PrimeScript™ RT Enzyme Mix I, and oligo dT primer using the protocols of the PrimeScriptTM RT Perfect Real-Time Reagent Kit (TaKaRa Bio, Japan). Subsequently, RT-qPCR was conducted using the SYBR® Green PCR Master Mix Kit (Applied Biosystems, USA), 10 ng of cDNA template, and 10 μM target gene primers. The cartilage related genes, including COL2, AGG, and SOX9, were analyzed by normalizing to the housekeeping gene glyceraldehyde-3-phosphate dehydrogenase (GAPDH). Sequences of the primers used are listed in table 1. Primer sequences used for RT-qPCR are summarized in table 1. The RT-qPCR conditions were 95 °C for 10 min and 40 cycles of 95 °C for 15 s, 60 °C for 1 min, and 95 °C for 15 s, with a final step of 60 °C for 1 min and 95 °C for 15 s. The results were analyzed using the Step One Plus™ Real-Time PCR system (Thermo Fisher Scientific). The melting curves were obtained to confirm the specificity of the amplified products, including the GAPDH housekeeping gene.

2.9. Statistical analyses

For the determination of statistical significance, the results were analyzed using a two-way analysis of variance (ANOVA) followed by Tukey's multiple comparison tests with every other sample group. A P-value < 0.05 was determined to be statistically significant. For quantitative data, the values are expressed as mean standard deviation.

3. Results and discussion

3.1. Fabrication of PDMS goblet-wells filled with Pluronic F-127

We successfully fabricated a 10 × 10 goblet-well substrate (well diameter 600 μm, hole diameter 300 μm) on PDMS. Using a uniform size of micro-pin and microbeads, goblet-wells were obtained (figure 3) and the uniform shapes were confirmed with SEM (figure S5). The metal beads were placed on the pre-patterned holes of the PDMS substrate to produce the goblet shape of each microwell. Holes of the goblet-wells were filled with Pluronic F-127 to stabilize the formation of spheroids (figures 3(d)–(f)). The presence of the Pluronic F-127 gel was confirmed by the safranin-O staining method. The red color dye was trapped inside the Pluronic F-127, as shown in figure S6. The filling was performed at a low temperature due to the sol–gel properties of Pluronic F-127. At low temperature, the gel-like Pluronic F-127 can reversibly change to a liquid state and thus flow throughout the hole in each well. When the temperature is subsequently increased, micelles of Pluronic F-127 form and the gel-like preparation is sequestered in the holes [32–34]. Temperature-responsive Pluronic hydrogels have been studied as mediators for the delivery of proteins or injectable cell therapeutic agents in the biopharmaceutical field. Pluronic hydrogels have characteristics that include minimal cell adhesion, minimal mechanical properties, and rapid erosion, which can be applied to tissue engineering or drug delivery [32, 35]. The attribute of minimal cell adhesion has been studied recently. Cell adhesion and protein adsorption are reportedly reduced on surfaces treated with Pluronic hydrogel [25, 36, 37]. This function supports spheroid formation at the initial stage, after which, the hydrogel degrades over time [38]. The goblet-wells also provide a better environment for biomolecule delivery.

3.2. Diffusion test

To visualize diffusion inside the holes connected to the goblet-well, we performed a computational simulation and measured the cross-section of the goblet-well interior by optical microscopy. In the experiment, the diffusion of Trypan blue at the bottom was observed in real-time, and simulation data were obtained under the same conditions (figure 4). The simulation data were set to display an area of 5% to 100% based on the mass ratio of the water (or cytokine) spread on the bottom surface (figure 4(a)), and the legend was set as blue so that it could be compared with the water-filled

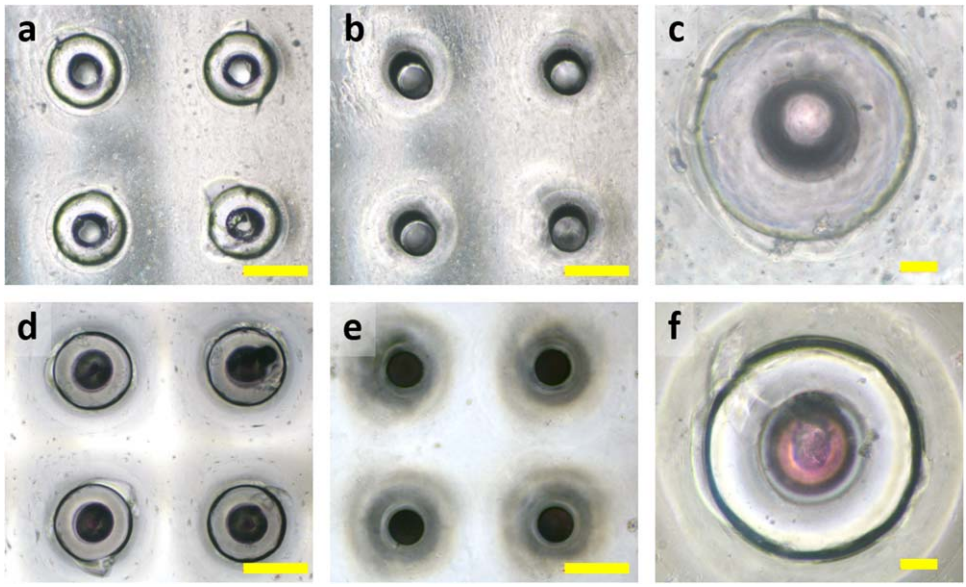

Figure 3. Optical microscopy images of goblet-wells fabricated using a micro-pin mold and microbeads. (a–c) Representative wells illustrating the goblet-wells with uniform size of the hemispherical wells and holes in the absence of Pluronic gel. (d–f) Microwells and holes filled with Pluronic gel (shown in red in panel f). The scale bars are 600 μm in a, b, d, and e, and 100 μm in c and f.

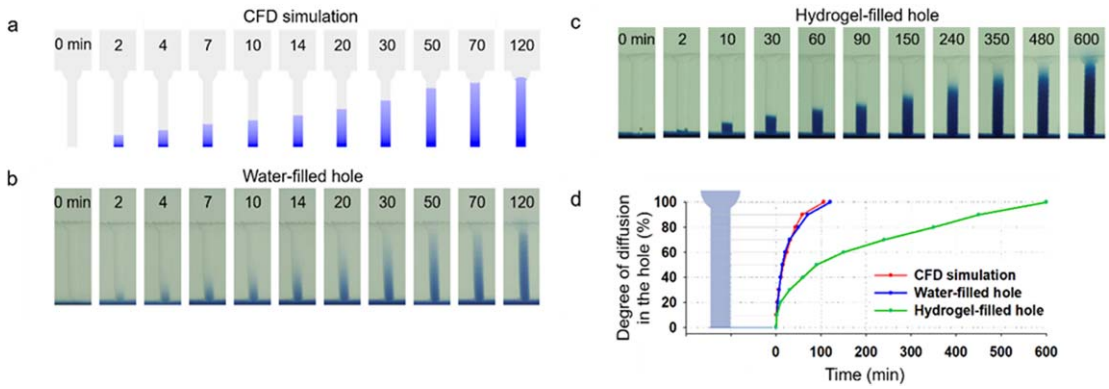

Figure 4. Computational analysis and empirical test to quantify the diffusion in holes of goblet-wells. (a) Computational diffusion model of water-filled holes. The medium of the bottom layer is shown in blue, and the mass fraction is displayed in blue until 5%. The process is divided into ten equal parts, and the numbers in the figure represent minutes. (b) Diffusion experimentation of water-filled holes. When the inside of the hole is filled with water, it takes approximately 120 min to transfer the medium from the bottom layer to the top layer. (c) Diffusion test of hydrogel-filled holes. When the inside of the hole is filled with hydrogel, it takes approximately 600 min to transfer the media from the bottom layer to the top layer. (d) Comparison of diffusion experiment and diffusion simulation data. When the hole is filled with water, the error between the experimental result and the simulation result is less than 10%. The diffusion in the hole filled with the hydrogel was approximately five times slower than diffusion in the hole filled with water.

hole experimental data. In each experiment, the area of the hole was divided into 10 equal zones and the time at which Trypan blue reached each zone from the bottom of the hole was determined. When the inside of the hole was filled with water (figure 4(b)), it took approximately 2 h for the Trypan blue to diffuse from the bottom to the top layer. The results of the simulation were similar to those of actual water diffusion (figure 4(d)) with an error rate $<10\%$. When the inside of the hole was filled with Pluronic F-127 (figure 4(c)), Trypan blue diffusion from the bottom to the top layer was five times longer, being completed within 10 h. Even though the diffusion rate of the hydrogel was slower than the diffusion rate of water, it was still applicable to a variety of spheroid co-culture and mass transfer systems, since diffusion was completed within 10 h. The diffusion time through the hole varied from 2 to up to 10 h, and could be adjusted according to the type and characteristics of the hydrogel. Since Pluronic F-127 can be degraded in nature [38], the diffusion rate after one point would become normal, similar to water diffusion, which would accelerate growth factor delivery when spheroids need more than initial state due to differentiation process.

3.3. Cell spheroid formation

We confirmed that the hASC spheroids formed stably depending on the Pluronic F-127 in goblet-wells. The

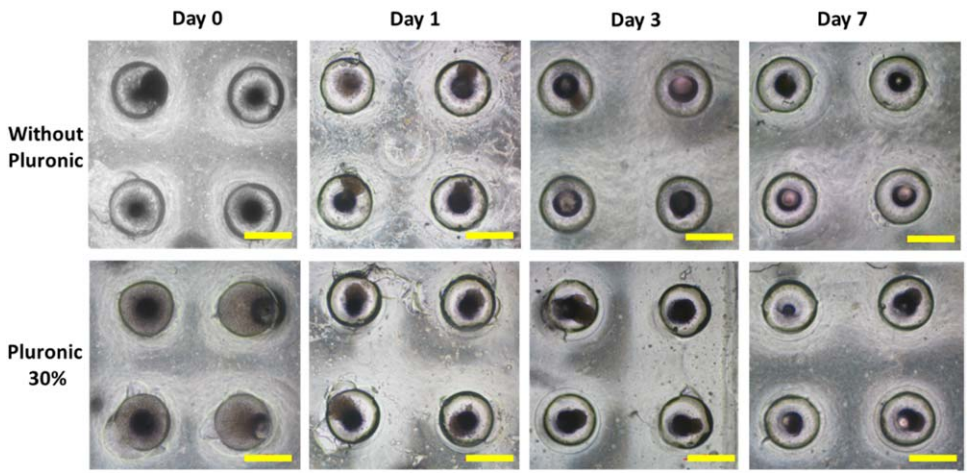

Figure 5. hASC spheroid formation in the goblet-wells that are not filled or filled with Pluronic F-127 after 0, 1, 3, and 7 d of cell culture. The spheroid cells were maintained stably until day 7 by goblet-well with Pluronic F-127. The scale bar is 600 μm.

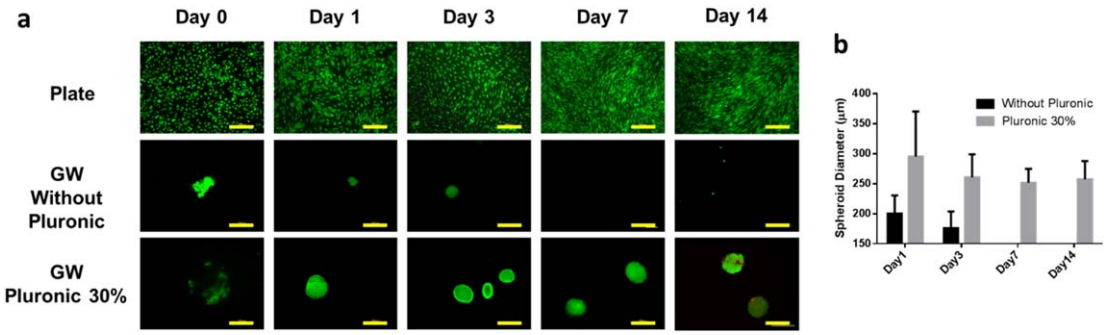

Figure 6. Cell vitality and size. (a) Live/Dead images of hASCs on the 6-well plates and the goblet-wells at days 0, 1, 3, 7, and 14 of cell culture. The goblet-wells either contained no or 30% Pluronic F-127. The scale bar is 300 μm. (b) The spheroid average diameter of hASCs on the goblet-well at days 1, 3, 7, and 14 d of cell culture.

hASCs were cultured in sterilized goblet-wells and the formation of spheroids was confirmed over time. The hASC spheroids formed stably and did not fall through the holes when the goblet-wells contained Pluronic F-127 gel (figure 5). The results at day 0 indicated that more cells were maintained in goblet-wells with Pluronic F-127 than in wells without gel. The comparison with goblet-wells without gel revealed that hASCs had not adhered to PDMS in the presence of Pluronic F-127 on day 1 [25–27]. Optical microscopy showed that the stable morphology of spheroids was maintained for a week, which was confirmed by Live/Dead imaging and staining with 4′, 6-diamidino-2-phenylindole and Rhodamine (see figures S1 and S2 in the supplementary material which is available online at stacks.iop.org/BF/12/015019/mmedia). Moreover, the proliferation rate of the spheroids was confirmed over 7 d culture, and we found the cells had proliferated (see figure S3 in the supplementary material).

3.4. Viability of hASC spheroids

The viability of hASC spheroids cultured in goblet-wells was determined. Most of the spheroids were alive (green) and only a few cells had died (red color in figure 6(a)). The validation of anoikis, an apoptosis at initial stage, also showed lower Ethidium homodimer signals compared to conventional control (figure S3). These results indicated that spheroids cultured in goblet-wells did not develop the necrosis that can occur in the central part of spheroids [39]. The necrotic core forms because of the limitation of the nutrient supply to the core and is commonly reported in spheroids with a diameter >500 μm [40, 41]. In our study, the average size of spheroids was <300 μm because the height of the well was 300 μm and, therefore, necrotic core formation was restricted. The average size of spheroids in goblet-wells containing 30% Pluronic F-127 was 295 $\pm$ 68 μm on day 1, 260 $\pm$ 35 μm on day 3, 251 $\pm$ 21 μm on day 7, and 257 $\pm$ 28 μm on day 14 (figure 6(b)). Spheroid size has been related to the aggregation and proliferation of the cells [16, 42]. The size of the spheroids in the presence of 30% Pluronic F-127 initially decreased (figure 6(b)) because cell aggregation was more pronounced than proliferation. After culturing for 3 d, spheroids entered the second phase, which featured excessive proliferation, followed by the third phase in

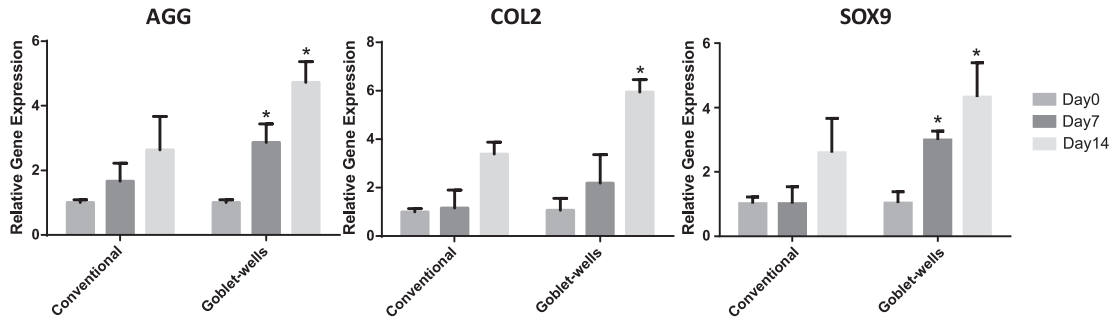

Figure 7. RT-qPCR results of each chondrogenic marker gene compared with GAPDH expression to assess the chondrogenic differentiation of hASCs in goblet-wells compared to conventional microwell at 14 d of cell culture (a) AGG; Aggrecan, (b) COL2; Type II collagen, and (c) SOX9; transcription factor. The expression of every gene was higher in cells in goblet-wells than in cells in conventional microwell at day 14 of cell culture ($^{*}P < 0.05$ compared to conventional microwell).

which the volume of the spheroid biomass stabilized after 10 d due to quiescent cells [42]. Corresponding with the 4′,6-diamidino-2-phenylindole/Rhodamine-stained spheroids (figure S2), actin (which is stained red by Rhodamine) seemed to be more centrally localized in the spheroids, which may indicate quiescent cells. For goblet-wells without gel, cells were flush away through the holes after day 1, therefore spheroid cannot be formed properly, corresponding with Live/Dead assay results obtained after day 7 when only separated cells remained. Due to the pronounced hydrophobicity of Pluronic F-127, cell assembly was more extensive and spheroids were more stable than the cells in goblet-wells without gel [16, 43, 44]

3.5. Chondrogenic differentiation of hASCs in goblet-wells

Because they can differentiate into various mesenchymal-type cells with therapeutic potential, hASCs can be used in tissue engineering and immune-modulatory applications [7, 45–47]. Based on this background, hASCs were cultured in 2D (6-well plates) and 3D (goblet-wells) conditions. To confirm the quantitative analysis of chondrogenic differentiation, RT-qPCR was performed to evaluate gene expression levels of AGG, COL2, and SOX-9 (figure S4). The expression of the three genes in 3D culture was higher than in 2D culture at days 7 and 14. It has been shown that spheroid cultures have the ability to enhance chondrogenic differentiation compared to 2D cell cultures [48–50]. To show the novelty of goblet-wells, the conventional microwells were used as a control to compare the chondrogenic differentiation (figure 7). The AGG gene, which is related to cell aggregation, was up-regulated in goblet-wells because the system provides more area for spheroids, allowing them to absorb more of the surrounding nutrient for differentiation. The all-around contact system of the goblet-well provides an *in vivo*-like environment, supporting cell interaction and aggregation [51]. The increased SOX9 gene expression in spheroids reflected the activation of HF-1α induced by the cell response to low oxygen diffusion in spheroids. This activation stimulates the production of SOX9 [15]. The SOX9 gene has a regulatory role in chondrogenesis, and it is the regulator of collagen type II (COL2), which is a key regulatory protein of cartilage [52]. Therefore, the up-regulation of COL2 is due to the high expression of SOX9. These results indicated that the chondrogenic differentiation levels of hASCs in goblet-wells were enhanced during 3D growth compared to those in conventional microwells. Several factors could affect the activation of differentiation, including the morphology of the *in vivo* cellular environment and the interaction between cells within a spherical shape [19, 53–55].

3.6. Chondrogenic differentiation of hASCs in goblet-wells with different treatments using chondrogenic medium

Biological signals in the form of growth factors are important in inducing cell differentiation toward the chondrogenic lineage [56]. We used different treatments with CDM for spheroids by diffusion through the bottom hole of each goblet-well. RT-qPCR examination of the expression of the AGG, COL2, and SOX9 target genes revealed increased expression of all three genes in all four conditions, with high expression at day 14 (figure 8). Expression of AGG and COL2 was highest in the CDM/CDM condition. In the GM/CDM condition, the gene expression was lower than in CDM/CDM because the growth factors in CDM at the bottom slowly diffuse to spheroids, and longer time is needed to reach the sufficient concentration for cell differentiation. By contrast, the CDM/GM condition displayed lower gene expression compared to CDM/CDM because of the initial high concentration of differentiation media, although it was diluted gradually by GM. Of note, when the concentration of ascorbic acid increases in media, the secretion of glycosaminoglycan (GAG) can decrease, implying a lower differentiation rate [57]. In addition, in the CDM/GM condition, the expression of every gene was higher compared to that in GM/CDM because the spheroids in the CDM/GM condition were exposed directly to the high concentration of CDM and thus had

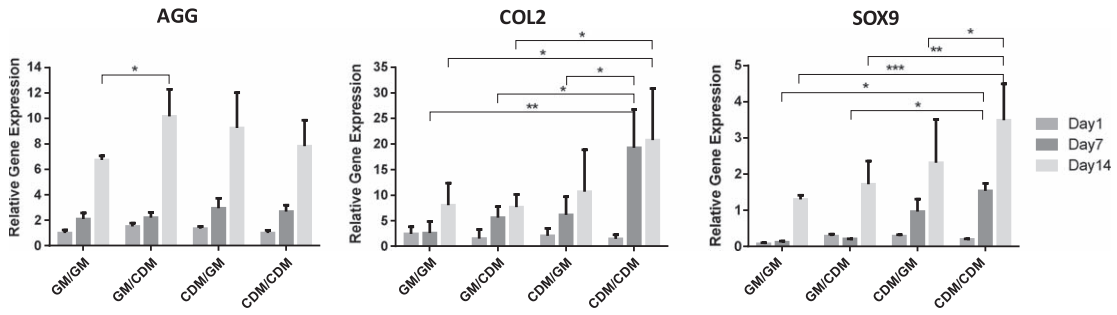

Figure 8. Schematic diagram of sample conditions and the relative gene expression of the chondrogenic marker genes (AGG, COL2, and SOX9). GAPDH is the housekeeping gene and its expression is normalized to cells at the time of spheroid formation. The expression was confirmed by qPCR analysis with chondrogenic differentiation of hASCs in goblet-well filled with Pluronic F-127. Four different combinations (in *x*-axis) of differentiation culture media were compared after 2 weeks of culture. ($^{*}P < 0.05$, $^{**}P < 0.005$, $^{***}P < 0.001$).

access to more supplements required for differentiation than in the GM/CDM condition. These results indicated that the growth rate of spheroids could be controlled by the diffusion rate of growth factors through the hole in a goblet-well. The presence of the growth factors can upregulate chondrogenic marker expression during 3D culture of cells [58]. This experiment using two different kinds of media, GM and CDM, demonstrated different growth rates, indicating the availability of a two-media phase for the co-culture of osteogenic and chondrogenic cells, which can be used as an *in vivo*-like system, mimicking osteochondral tissue. These gene expression results imply that our goblet-well system has the potential for *in vivo*-like spheroid cell co-culture with osteogenic cells by the biomolecule diffusion pathway. This system may be the basis of further advanced research on osteochondral tissue regeneration.

4. Conclusion

Using goblet-wells and Pluronic F-127, we devised a system capable of exposing spheroids to two different media/cytokines. Prolonged culture of the spheroids was successful. The spheroid culture system is a useful 3D cell culture system that results in similar functional and morphological features with cells *in vivo*. There are various ways to cultivate spheroids. The present system using micro-pin mold and beads is easy and cost-effective. In addition, goblet-wells having a uniform size prepared through micro-pin mold and beads were successfully used to cultivate hASC spheroids. Pluronic F-127 was used to reduce cell adhesion to the PDMS surface and to form hASC spheroids by filling the holes of the goblet-wells. Spheroids with a diameter <300 μm were cultured with very little cell death. The level of chondrogenic differentiation in the goblet-wells was improved compared to the 2D culture. Moreover, we checked the effect of diffusion and found that gene expression was controllable by varying the treatment pattern. This diffusion ability in the 3D cell co-culture platform will be useful for future investigations of 3D spheroid cell co-culture systems of chondrogenic cells (in which differentiation is enhanced; figure 7) and osteogenic cells for osteochondral tissue engineering. The results demonstrate the production of spheroids that can effectively regenerate cartilage tissue and have various applications, such as in drug or growth factor delivery systems and cell therapy.

Acknowledgments

This research was supported by Creative Materials Discovery Program through the National Research Foundation of Korea(NRF) funded by Ministry of Science and ICT(NRF-2018M3D1A1058813), the National Research Foundation of Korea (NRF) funded by Ministry of Science and ICT (NRF-2019R1A2C1007088), and the Bio & Medical Technology Development Program of the NRF funded by the Korean government, MSIT (2018M3A9H1023141).

ORCID iDs

Joong Yull Park https://orcid.org/0000-0002-0164-8701
Hansoo Park https://orcid.org/0000-0002-3125-7680

References

[1] Helmick C G, Felson D T, Lawrence R C, Gabriel S, Hirsch R, Kwoh C K, Liang M H, Kremers H M, Mayes M D and Merkel P A 2008 Estimates of the prevalence of arthritis and other rheumatic conditions in the United States: I. *Arthritis Rheumatism* **58** 15–25
[2] Carvalho M R, Reis R L and Oliveira J M 2018 Mimicking the 3D biology of osteochondral tissue with microfluidic-based solutions: breakthroughs towards boosting drug testing and discovery *Drug Discovery Today* **23** 711–8
[3] Carvalho M R, Reis R L and Oliveira J M 2018 Mimicking the 3D biology of osteochondral tissue with microfluidic-based solutions: breakthroughs towards boosting drug testing and discovery *Drug Discovery Today* **23** 711–8

[4] Lin H, Lozito T P, Alexander P G, Gottardi R and Tuan R S 2014 Stem cell-based microphysiological osteochondral system to model tissue response to interleukin-1β *Mol. Pharmaceutics* **11** 2203–12
[5] Tare R S, Howard D, Pound J C, Roach H I and Oreffo R O 2005 Tissue engineering strategies for cartilage generation–micromass and three dimensional cultures using human chondrocytes and a continuous cell line *Biochem Biophys. Res. Commun.* **333** 609–21
[6] Wang W, Itaka K, Ohba S, Nishiyama N, Chung U-I, Yamasaki Y and Kataoka K 2009 3D spheroid culture system on micropatterned substrates for improved differentiation efficiency of multipotent mesenchymal stem cells *Biomaterials* **30** 2705–15
[7] Wu L, Cai X X, Zhang S, Karperien M and Lin Y F 2013 Regeneration of articular cartilage by adipose tissue derived mesenchymal stem cells: perspectives from stem cell biology and molecular medicine *J. Cell. Physiol.* **228** 938–44
[8] Shim J-H, Lee J-S, Kim J Y and Cho D-W 2012 Bioprinting of a mechanically enhanced three-dimensional dual cell-laden construct for osteochondral tissue engineering using a multi-head tissue/organ building system *J. Micromech. Microeng.* **22** 085014
[9] van Duinen V, Trietsch S J, Joore J, Vulto P and Hankemeier T 2015 Microfluidic 3D cell culture: from tools to tissue models *Curr. Opin. Biotechnol.* **35** 118–26
[10] Imazato S, Sasaki J-I, Matsumoto T, Yatani H, Egusa H, Nishiguchi A, Matsusaki M, Akashi M and Nakano T 2012 *In vitro* reproduction of endochondral ossification using a 3D mesenchymal stem cell construct *Interact. Biol.* **4** 1207–14
[11] Murata D, Akieda S, Misumi K and Nakayama K 2018 Osteochondral regeneration with a scaffold-free three-dimensional construct of adipose tissue-derived mesenchymal stromal cells in pigs *Tissue Eng. Regen. Med.* **15** 101–13
[12] Cesarz Z and Tamama K 2016 Spheroid culture of mesenchymal stem cells *Stem Cells Int.* **2016** 9176357
[13] Tung Y C, Hsiao A Y, Allen S G, Torisawa Y S, Ho M and Takayama S 2011 High-throughput 3D spheroid culture and drug testing using a 384 hanging drop array *Analyst* **136** 473–8
[14] Fennema E, Rivron N, Rouwkema J, van Blitterswijk C and de Boer J 2013 Spheroid culture as a tool for creating 3D complex tissues *Trends Biotechnol.* **31** 108–15
[15] Yoon H H, Bhang S H, Shin J-Y, Shin J and Kim B-S 2012 Enhanced cartilage formation via three-dimensional cell engineering of human adipose-derived stem cells *Tissue Eng.* A **18** 1949–56
[16] Lee G-H, Park Y E, Cho M, Park H and Park J Y 2016 Magnetic force-assisted self-locking metallic bead array for fabrication of diverse concave microwell geometries *Lab Chip* **16** 3565–75
[17] Laschke M W and Menger M D 2017 Life is 3D: boosting spheroid function for tissue engineering *Trends Biotechnol.* **35** 133–44
[18] Choi Y Y, Chung B G, Lee D H, Khademhosseini A, Kim J-H and Lee S-H 2010 Controlled-size embryoid body formation in concave microwell arrays *Biomaterials* **31** 4296–303
[19] Kim B-C, Kim J H, An H J, Byun W, Park J-H, Kwon I K, Kim J S and Hwang Y-S 2014 Microwell-mediated micro cartilage-like tissue formation of adipose-derived stem cell *Macromol. Res.* **22** 287–96
[20] Hwang Y-S, Kim J, Yoon H J, Kang J I, Park K-H and Bae H 2018 Microwell-mediated cell spheroid formation and its applications *Macromol. Res.* **26** 1–8
[21] Khademhosseini A, Yeh J, Eng G, Karp J, Kaji H, Borenstein J, Farokhzad O C and Langer R 2005 Cell docking inside microwells within reversibly sealed microfluidic channels for fabricating multiphenotype cell arrays *Lab Chip* **5** 1380–6
[22] Lee S-A, Kang E, Ju J, Kim D-S and Lee S-H 2013 Spheroid-based three-dimensional liver-on-a-chip to investigate hepatocyte–hepatic stellate cell interactions and flow effects *Lab Chip* **13** 3529–37
[23] Abaci H E, Coffman A, Doucet Y, Chen J, Jacków J, Wang E, Guo Z, Shin J U, Jahoda C A and Christiano A M 2018 Tissue engineering of human hair follicles using a biomimetic developmental approach *Nat. Commun.* **9** 5301
[24] Mescher A L 2013 *Junqueira's Basic Histology: Text and Atlas* (New York : Mcgraw-Hill)
[25] Zheng J, Song W, Huang H and Chen H 2010 Protein adsorption and cell adhesion on polyurethane/Pluronic® surface with lotus leaf-like topography *Colloids Surf.* B **77** 234–9
[26] Boxshall K, Wu M H, Cui Z, Cui Z, Watts J F and Baker M A 2006 Simple surface treatments to modify protein adsorption and cell attachment properties within a poly (dimethylsiloxane) micro-bioreactor *Surf. Interface Anal.* **38** 198–201
[27] Wu M H 2009 Simple poly (dimethylsiloxane) surface modification to control cell adhesion *Surf. Interface Anal.* **41** 11–6
[28] Gao Y, Liu S, Huang J, Guo W, Chen J, Zhang L, Zhao B, Peng J, Wang A and Wang Y 2014 The ECM-cell interaction of cartilage extracellular matrix on chondrocytes *BioMed Res. Int.* **2014** 648459
[29] Miao L, Jianren S, Ying S, Christopher B and Quanfang C 2009 Thickness-dependent mechanical properties of polydimethylsiloxane membranes *J. Micromech. Microeng.* **19** 035028
[30] Koschwanez J H, Carlson R H and Meldrum D R 2009 Thin PDMS films using long spin times or tert-butyl alcohol as a solvent *PLoS One* **4** e4572
[31] Han Q, Bradshaw E M, Nilsson B, Hafler D A and Love J C 2010 Multidimensional analysis of the frequencies and rates of cytokine secretion from single cells by quantitative microengraving *Lab Chip* **10** 1391–400
[32] Chung Y-I, Lee S-Y and Tae G 2006 The effect of heparin on the gellation of Pluronic F-127 hydrogel *Colloids Surf.* A **284** 480–4
[33] Pandit N K and Kisaka J 1996 Loss of gelation ability of Pluronic® F127 in the presence of some salts *Int. J. Pharmaceutics* **145** 129–36
[34] Vadnere M, Amidon G, Lindenbaum S and Haslam J L 1984 Thermodynamic studies on the gel-sol transition of some pluronic polyols *Int. J. Pharmaceutics* **22** 207–18
[35] Lee Y, Chung H J, Yeo S, Ahn C-H, Lee H, Messersmith P B and Park T G 2010 Thermo-sensitive, injectable, and tissue adhesive sol–gel transition hyaluronic acid/pluronic composite hydrogels prepared from bio-inspired catechol-thiol reaction *Soft Matter* **6** 977–83
[36] Boxshall K, Wu M H, Cui Z, Cui Z, Watts J F and Baker M A 2006 Simple surface treatments to modify protein adsorption and cell attachment properties within a poly (dimethylsiloxane) micro-bioreactor *Surf. Interface Anal.: Int. J. Devoted Dev. Appl. Tech. Anal. Surf., Interfaces Thin Films* **38** 198–201
[37] Wu M H 2009 Simple poly (dimethylsiloxane) surface modification to control cell adhesion *Surf. Interface Anal.: Int. J. Devoted Dev. Appl. Tech. Anal. Surf., Interfaces Thin Films* **41** 11–6
[38] Diniz I M A, Chen C, Xu X, Ansari S, Zadeh H H, Marques M M, Shi S and Moshaverinia A 2015 Pluronic F-127 hydrogel as a promising scaffold for encapsulation of dental-derived mesenchymal stem cells *J. Mater. Sci. Mater. Med.* **26** 153
[39] Vadivelu R, Kamble H, Shiddiky M and Nguyen N-T 2017 Microfluidic technology for the generation of cell spheroids and their applications *Micromachines* **8** 94
[40] Mosaad E O, Chambers K F, Futrega K, Clements J A and Doran M R 2018 The Microwell-mesh: a high-throughput 3D prostate cancer spheroid and drug-testing platform *Sci. Rep.* **8** 253
[41] Hirschhaeuser F, Menne H, Dittfeld C, West J, Mueller-Klieser W and Kunz-Schughart L A 2010 Multicellular tumor spheroids: an underestimated tool is catching up again *J. Biotechnol.* **148** 3–15
[42] Ziolkowska K, Stelmachowska A, Kwapiszewski R, Chudy M, Dybko A and Brzozka Z 2013 Long-term three-dimensional cell culture and anticancer drug activity evaluation in a microfluidic chip *Biosens. Bioelectron.* **40** 68–74
[43] Ko D Y, Patel M, Lee H J and Jeong B 2018 Coordinating thermogel for stem cell spheroids and their cyto-effectiveness *Adv. Funct. Mater.* **28** 1706286

[44] Shen K, Lee J, Yarmush M L and Parekkadan B 2014 Microcavity substrates casted from self-assembled microsphere monolayers for spheroid cell culture *Biomed. Microdevices* **16** 609–15
[45] Beeson W, Woods E and Agha R 2011 Tissue engineering, regenerative medicine, and rejuvenation in 2010: the role of adipose-derived stem cells *Facial Plast. Surg.* **27** 378–87
[46] Dai R, Wang Z, Samanipour R, Koo K I and Kim K 2016 Adipose-derived stem cells for tissue engineering and regenerative medicine applications *Stem Cells Int.* **2016** 6737345
[47] Wankhade U D, Shen M, Kolhe R and Fulzele S 2016 Advances in adipose-derived stem cells isolation, characterization, and application in regenerative tissue engineering *Stem Cells Int.* **2016** 3206807
[48] Lach M S, Wroblewska J, Kulcenty K, Richter M, Trzeciak T and Suchorska W M 2019 Chondrogenic differentiation of pluripotent stem cells under controllable serum-free conditions *Int. J. Mol. Sci.* **20** 2711
[49] Merceron C, Portron S, Masson M, Lesoeur J, Fellah B H, Gauthier O, Geffroy O, Weiss P, Guicheux J and Vinatier C 2011 The effect of two- and three-dimensional cell culture on the chondrogenic potential of human adipose-derived mesenchymal stem cells after subcutaneous transplantation with an injectable hydrogel *Cell Transplant.* **20** 1575–88
[50] Sridharan B, Laflin A D and Detamore M S 2018 Generating chondromimetic mesenchymal stem cell spheroids by regulating media composition and surface coating *Cellular Mol. Bioeng.* **11** 99–115
[51] Foldager C B, Nielsen A B, Munir S, Ulrich-Vinther M, Søballe K, Bünger C and Lind M 2011 Combined 3D and hypoxic culture improves cartilage-specific gene expression in human chondrocytes *Acta Orthopaedica* **82** 234–40
[52] Healy C, Uwanogho D and Sharpe P T 1999 Regulation and role of Sox9 in cartilage formation *Dev. Dyn.* **215** 69–78
[53] Ichinose S, Tagami M, Muneta T and Sekiya I 2005 Morphological examination during *in vitro* cartilage formation by human mesenchymal stem cells *Cell Tissue Res.* **322** 217–26
[54] Sébastien S, Ang-Chen T, Yan L and Teng M 2014 Three-dimensional aggregates of mesenchymal stem cells: cellular mechanisms, biological properties, and applications *Tissue Eng.* B **20** 365–80
[55] Winter A, Breit S, Parsch D, Benz K, Steck E, Hauner H, Weber R M, Ewerbeck V and Richter W 2003 Cartilage-like gene expression in differentiated human stem cell spheroids: a comparison of bone marrow–derived and adipose tissue–derived stromal cells *Arthritis Rheumatism* **48** 418–29
[56] Awad H A, Halvorsen Y-D C, Gimble J M and Guilak F 2003 Effects of transforming growth factor β1 and dexamethasone on the growth and chondrogenic differentiation of adipose-derived stromal cells *Tissue Eng.* **9** 1301–12
[57] Barlian A, Judawisastra H, Alfarafisa N M, Wibowo U A and Rosadi I 2018 Chondrogenic differentiation of adipose-derived mesenchymal stem cells induced by L-ascorbic acid and platelet rich plasma on silk fibroin scaffold *PeerJ* **6** e5809-e
[58] Hwang N S, Kim M S, Sampattavanich S, Baek J H, Zhang Z and Elisseeff J 2006 Effects of three-dimensional culture and growth factors on the chondrogenic differentiation of murine embryonic stem cells *Stem Cells* **24** 284–91